

5-7-1994

## Conventional and High Resolution Scanning Electron Microscopy and Cryofracture Techniques as Tools for Tracing Cerebellar Short Intracortical Circuits

Orlando J. Castejón  
*Universidad del Zulia, Venezuela*

Robert P. Apkarian  
*Emory University*

Consuelo Valero  
*Universidad del Zulia, Venezuela*

Follow this and additional works at: <https://digitalcommons.usu.edu/microscopy>



Part of the [Biology Commons](#)

---

### Recommended Citation

Castejón, Orlando J.; Apkarian, Robert P.; and Valero, Consuelo (1994) "Conventional and High Resolution Scanning Electron Microscopy and Cryofracture Techniques as Tools for Tracing Cerebellar Short Intracortical Circuits," *Scanning Microscopy*. Vol. 8 : No. 2 , Article 14.

Available at: <https://digitalcommons.usu.edu/microscopy/vol8/iss2/14>

This Article is brought to you for free and open access by the Western Dairy Center at DigitalCommons@USU. It has been accepted for inclusion in Scanning Microscopy by an authorized administrator of DigitalCommons@USU. For more information, please contact [digitalcommons@usu.edu](mailto:digitalcommons@usu.edu).



## CONVENTIONAL AND HIGH RESOLUTION SCANNING ELECTRON MICROSCOPY AND CRYOFRACTURE TECHNIQUES AS TOOLS FOR TRACING CEREBELLAR SHORT INTRACORTICAL CIRCUITS

Orlando J. Castejón\*, Robert P. Apkarian<sup>1</sup> and Consuelo Valero

Instituto de Investigaciones Biológicas, Facultad de Medicina, Universidad del Zulia, Maracaibo, Venezuela

<sup>1</sup>Yerkes Regional Research Center, Emory University, Atlanta, Georgia, U.S.A.

(Received for publication December 31, 1993 and in revised form May 7, 1994)

### Abstract

The present paper shows the potential contribution of conventional and high resolution scanning electron microscopy (SEM) to trace short intracortical circuits in cryofractured fish, primate and human cerebelli. Conventional SEM slicing technique allowed us to identify afferent mossy and climbing fibers and their synaptic relationship in the granular layer. SEM freeze-fracture method exposed the mossy glomerular synapses and the axo-dendritic connections of climbing fibers. At the Purkinje cell layer, the cryofracture process removed the satellite Bergmann glial cell layer, displaying a partial view of the supra- and infra-ganglionic plexuses of Purkinje cells and the ascending pathways of climbing fibers. High resolution SEM (HRSEM) showed the specimen specific secondary electron (SE-I) image of axosomatic synapses on Golgi cell surface. At the molecular layer, the outer surface of parallel fiber synaptic varicosities were distinguished, establishing the cruciform *en passant* synaptic contact with the Purkinje cell dendritic spines. HRSEM showed the fractured parallel fiber synaptic varicosities containing spheroidal synaptic vesicles embedded in a high dense extravesicular material. Conventional SEM and gold-palladium coating are useful to trace intracortical circuits. With HRSEM and chromium coating, it is possible to study the outer and inner surfaces of synaptic connections.

**Key Words:** Scanning electron microscopy, nerve circuits, synapses.

\*Address for correspondence and present address:  
Orlando J. Castejón,  
Mision Permanente de Venezuela aupres ONU,  
18 A Francois Lehmann  
CH-1218 Grand Saconnex, Geneve,  
Switzerland

Telephone number: (41) 22 798 2621  
FAX number: (41) 22 798 5877

### Introduction

Cryofractured teleost fish, primate and human cerebelli were processed for conventional scanning electron microscopy (SEM) and high resolution scanning electron microscopy (HRSEM) in an attempt to characterize cerebellar afferent fibers (climbing and mossy fibers) and their intracortical neuronal relationship, as well as to identify short intracortical circuits, such as granule cell (parallel fiber) and stellate cell axons-Purkinje cell relationship. Intracortical circuits have been classically described with Golgi light microscopy (Scheibel and Scheibel, 1954; Ramón y Cajal, 1955), transmission electron microscopy (TEM) (Palay and Chan-Palay, 1974), computer aided methods, injection of vital stains, electrophysiological recordings, and immunocytochemical methods (Llinas and Hillman, 1969; Kuffler *et al.*; 1984; Shepher, 1988). However, until now, very few attempts have been made to trace intracortical circuits with SEM and HRSEM (Lewis, 1971; Castejón, 1981). The cryofracture method for SEM (Haggis, 1970; Humphreys *et al.*, 1974) applied to the brain tissue (Castejón, 1984, 1986, 1988, 1990 a,b, 1993; Castejón and Apkarian, 1992) allowed us to visualize, in the cerebellum, the cytoarchitectonic arrangement or layered structure of a gray center (Castejón and Caraballo, 1980; Castejón and Valero, 1980) and to explore neuronal geometry *in situ* (Castejón, 1991) thereby examining outer and inner surfaces of synaptic contacts (Castejón and Apkarian, 1993).

The aim of the present paper is to show the potential contribution of scanning electron microscopy and the cryofracture method for obtaining new information on the three-dimensional hidden relationships between the extrinsic afferent fibers (climbing and mossy fibers) and the cerebellar nerve cells and also to show how the scanning electron microscope probe could be used to trace through a three-layered structure such as the intrinsic cerebellar circuits, formed by the parallel fibers and Purkinje cell dendrites.

## Material and Methods

### Slicing technique for conventional SEM (Castejón and Caraballo, 1980)

Specimens of teleost fishes, *Arius spixii*, weighing 30-32 g and kept in aquaria at room temperature, were used. Pieces of tissue were fixed: 1) by immersion in 5% glutaraldehyde in 0.1 M phosphate buffer, pH 7.4; or 2) by vascular perfusion with 4% glutaraldehyde in 0.1 M phosphate buffer solution, pH 7.4; or 3) by immersion in Karnovsky fixative. Slices of 2-3 mm thickness were cut with a razor blade and fixed overnight in the same buffered fixative. After washing in buffered saline, the tissue blocks were dehydrated through graded concentrations of ethanol, dried by the critical point (CPD) method with liquid CO<sub>2</sub> as recommended by Anderson (1951), mounted on copper stubs, and coated with carbon and gold-palladium. The specimens were examined in a JEOL JEM 100B electron microscope, equipped with ASID scanning attachment, operated at an accelerating voltage of 20 kV.

### Freeze-fracture for conventional SEM (Castejón, 1981)

This method was applied to study the cerebellar cortex of two teleost fishes: *Arius spixii* and Salmo trout. After Karnovsky fixation, cerebellar slices, 2-3 mm thick, were cut with a razor blade and fixed by immersion in the same fixative for 4-5 hours. After washing in buffered saline, they were postfixed in 1% osmium tetroxide in 0.1 M phosphate buffer solution, pH 7.4, for 1 hour. After rinsing in a similar buffer, tissue blocks were dehydrated through graded concentrations of ethanol, rapidly frozen by plunging into Freon 22, cooled by liquid nitrogen (Haggis, 1970; Haggis and Phipps-Todd, 1977) and fractured with a precooled razor blade. The tissue was then dried by the critical point method with liquid CO<sub>2</sub> and coated with gold-palladium. Specimens were examined in the same JEOL JEM 100B EM-ASID operated at an accelerating voltage of 80 kV.

### Conventional SEM and cryofracture technique of human cerebelli (Castejón and Valero, 1980)

Seven human cerebelli obtained from young people (11-25 years), who died by drowning or non-neurological diseases were used in the present study. The cerebellum was removed at the autopsy 4 to 11 hours after death. Macroscopically, the cerebellum showed anoxic changes and moderate brain edema. Small samples of cerebellar cortex, 3-5 mm thick, were processed according to the technique of Humphreys *et al.* (1974, 1975) with minor modifications (using phosphate buffer instead of cacodylate buffer). The samples were fixed for 2 to 16 hours in 4% glutaraldehyde-phosphate buffer solution, 0.1 M, pH 7.4, dehydrated in ethanol and frozen

in liquid nitrogen (LN<sub>2</sub>). The fracture was made with a precooled razor blade and the fragments placed in ethanol at room temperature for thawing. The critical point drying was done with liquid CO<sub>2</sub> followed by a coating of carbon or gold-palladium in a JEOL JEE-46 high vacuum evaporator. The tissue was observed with same JEOL JEM 100B EM-ASID.

### Nerve tissue fixation for HRSEM (Castejón and Apkarian, 1992)

Upon intracardial cannulation juvenile rhesus monkey cerebellar cortex was flushed with Ringer lactate buffer and then perfused fixed with 4% paraformaldehyde and 0.1% glutaraldehyde in 0.05% phosphate buffer, pH 7.4. Prior to excision a perfusion of 5% buffered sucrose cleared all upper body vasculature.

Excised rhesus cerebellar cortex was minced into 2 mm<sup>3</sup> pieces and further fixed in 2.5% electron microscopy (EM) grade glutaraldehyde in 0.1 M cacodylate buffer, pH 7.4, overnight in order to provide complete intracellular proteinaceous cross-linking. Cacodylate buffer, pH 7.4, was used to completely remove the primary fixative by rinsing the tissue several times under gentle agitation. Postfixation of phospholipid moieties was accomplished by immersion in 1% OsO<sub>4</sub> in 0.1 M cacodylate buffer, pH 7.4, for one hour and then rinsed in cacodylate buffer several times.

### Delicate specimen preparation

A graded series of ethanols (30, 50, 70, 80, 90, 2x100%) was used to substitute tissue fluids prior to wrapping individual tissue pieces in preformed absolute ethanol filled parafilm cryofracture packets. Rapid freezing of packets was performed by plunging into Freon-22 at its melting point (-155°C) and then stored in LN<sub>2</sub>. A modified tissue chopper (Sorvall TC-2) equipped with a LN<sub>2</sub> copper stage and a precooled fracture blade (-196°C) was utilized for cryofracture. First, the packet was transferred from the LN<sub>2</sub> storage vessel with LN<sub>2</sub> chilled forceps in order to avoid thermal damage. Secondly, the cooled fracture blade was raised from the LN<sub>2</sub>, the packet was orientated under the blade, and the arm was immediately activated to strike only the top of the packet (Apkarian and Curtis, 1986). Fractured tissue fragments were transferred into chilled absolute ethanol (4°C) and thawed. Tissues were loaded into fresh absolute ethanol filled mesh baskets within the boat of a Polaron E-3000 critical point dryer, the boat loaded into the dryer, and exchange with CO<sub>2</sub> gas at a rate of 1.2 l/min. The CPD chamber was then thermally regulated to the critical temperature and pressured at a rate of 1°C/min. Following the phase transition, the CO<sub>2</sub> gas was released at a gas flow rate of 1.2 l/min. (Peters, 1980). Dried specimens, shiny face up, were mounted onto aluminum stubs 9 mm x 2 mm x 1 mm

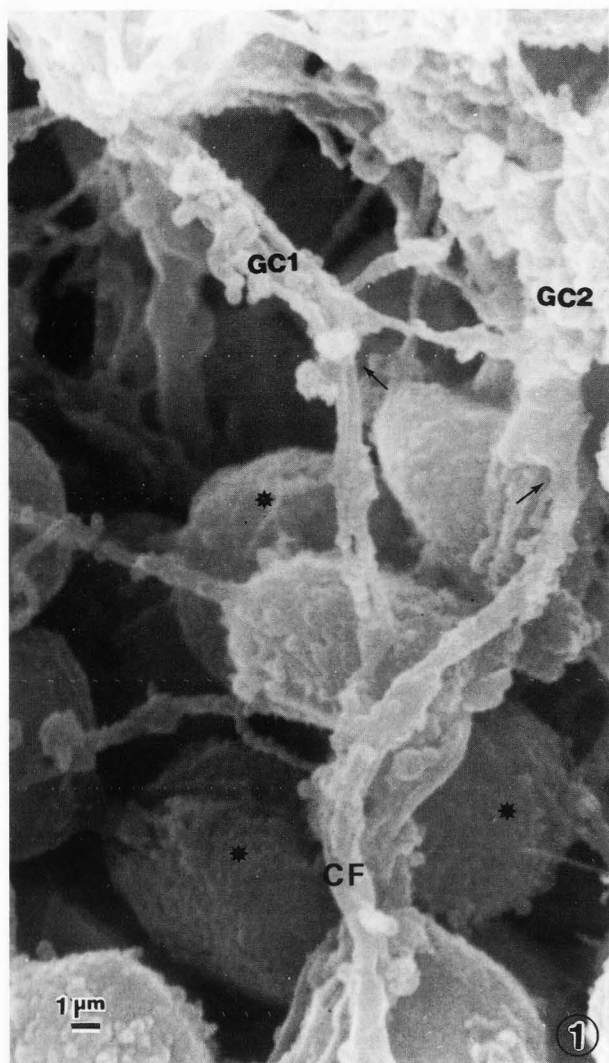


**Figure 1.** Teleost fish cerebellar granule cell layer. Thin parent climbing fibers (CF) establishing 1 to 1 axo-dendritic contacts with granule cell (GC1, GC2) dendrites at the sites indicated by arrows. The large depth of focus of SEM allows us to appreciate the underlying granule cells (asterisks). SEM slicing technique. Gold-palladium coating.

for the ISI DS-130 SEM upper stage or onto brass mounts for the Hitachi S-900 SEM with silver paste and degassed at  $5 \times 10^{-7}$  torr prior to coating.

#### Metal coating for HRSEM imaging

Dried and mounted specimens were chromium coated with a continuous 2 nm film in a Denton DV-602 turbo pumped sputter deposition system operated in a vacuum of Argon at  $5 \times 10^{-3}$  torr (Apkarian, 1994).

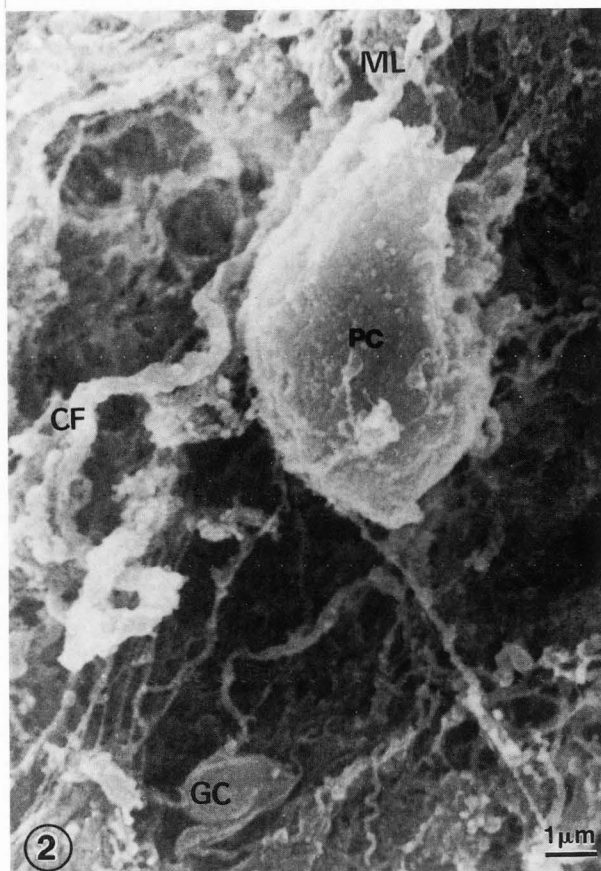


**Figure 2.** Teleost fish Purkinje cell layer. The climbing fibers (CF) are observed leaving the granule cell (GC) layer, approaching the Purkinje cell body (PC) and ascending toward the molecular layer (ML). SEM slicing technique. The Bergmann glial cell cytoplasm ensheathing the Purkinje cell has been removed during the SEM slicing procedure, thereby allowing visualization of intracortical course of climbing fiber and Purkinje cell outer surface.

#### Scanning electron microscopy (SEM)

Specimens were introduced onto the condenser/objective (C/O) lens stages (predominantly primary beam generated secondary electron, SE-I, signal mode operation) of either an ISI DS-130 equipped with LaB<sub>6</sub> emitter or a Hitachi S-900 SE equipped with a cold cathode field emitter. Both instruments were operated at accelerating voltages of 25-30 kV in order to produce minimal spot size and adequate signal to noise ratio at all magnifications. Micrographs were focus printed to reduce instrumental noise (Peters, 1985).

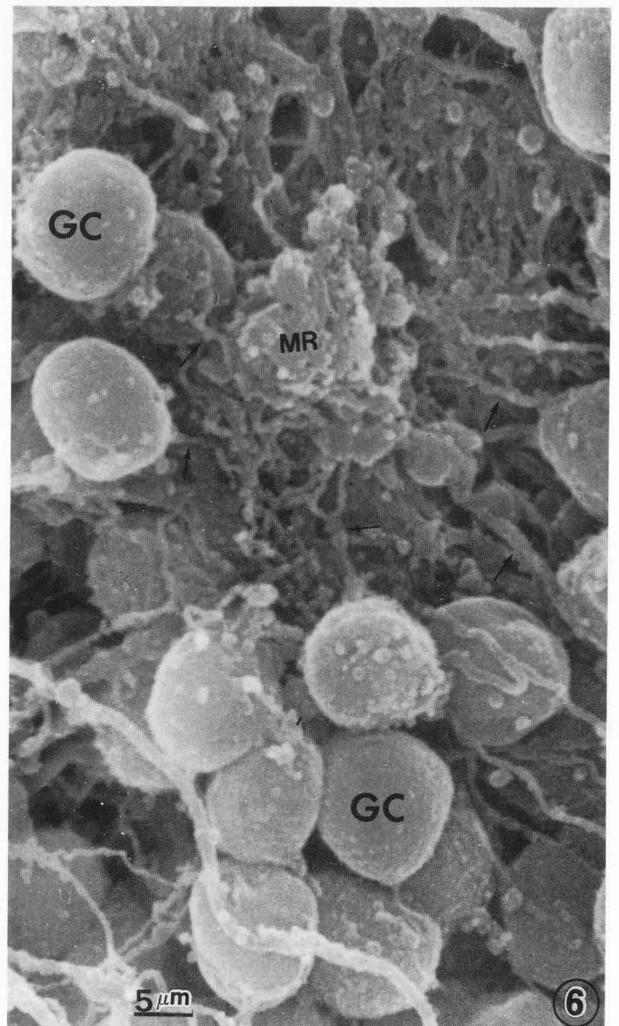
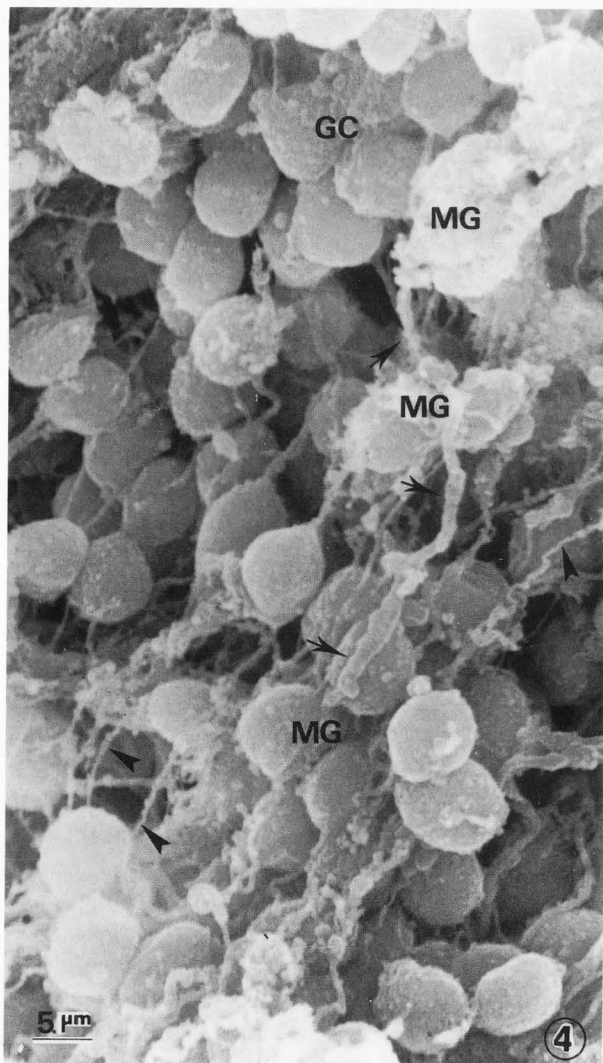
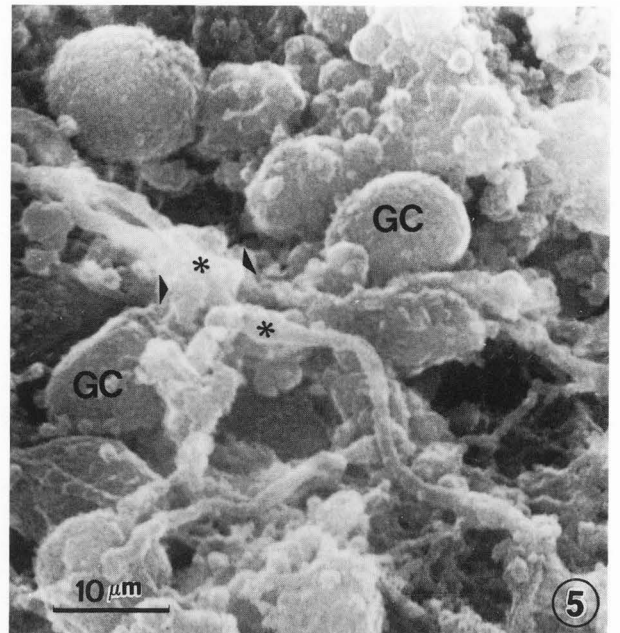
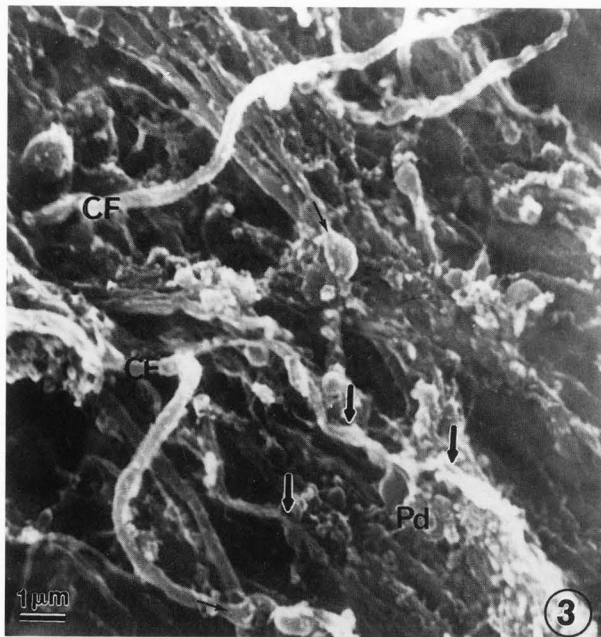


**Figure 3.** Teleost fish cerebellar cortex. Molecular layer. Climbing fibers (CF) are seen ending (arrows) on the outer surface of Purkinje dendritic branches (Pd) by means of bulbous endings (thin arrows). SEM slicing technique. Gold-palladium coating.

**Figure 4.** Teleost fish cerebellar cortex. Granule cell layer. Thick parent mossy fibers (arrows) are observed crossing the granule cell (GC) layer and establishing *en passant* mossy glomerular (MG) contacts with several granule cell groups. Fine identified fibers (arrowheads) are observed dispersed throughout the granular layer; they may correspond to fine collaterals of mossy fibers, climbing collaterals, or Golgi cell axonal ramifications. SEM slicing technique. Gold-palladium coating.

**Figure 5.** Teleost fish cerebellar cortex. Granule cell layer. Fractured mossy fiber glomerulus showing the central mossy fiber rosette (asterisks) surrounded by granule cell (GC) dendritic processes (arrowheads). Freon freeze-fracture method. Gold-palladium coating.

**Figure 6.** Fractured mossy fiber glomerulus showing up to 18 granule cells (GC) surrounding a central mossy rosette (MR). Note the granule cell dendritic processes (arrows) converging radially to the mossy rosette. Freon freeze-fracture method. Gold-palladium coating.

## Results

### SEM slicing technique

Examination at low magnification of the cerebellar white matter processed according to the slicing technique showed the afferent fibers entering into the granular layer. At higher magnification, close scrutiny of the granular layer showed bundles of thin parent fibers approaching the granule cell groups. These thin fibers gave off fine collateral tendrils, which spread toward the neighboring granule cell groups. The parent fibers were observed establishing contact with granule cell dendrites. At a higher magnification of the granular layer, the granule cell processes, both dendrites and axon, were clearly distinguished as well as their topographic relationship with the afferent fibers. Close examination of these contacts allowed us to characterize axo-dendritic relations between climbing fibers and granule cell dendrites in a ratio of 1 to 1 (Fig. 1).

Ascending to the Purkinje cell layer, we observed how the unbranched parent fibers approached the Purkinje cell body (Fig. 2) on their way to the molecular layer. In this layer, they were observed ascending toward the surface of the cerebellar folia along the surface of Purkinje cell dendrites and emitting ascending, transverse and descending collateral processes. These collateral processes were observed passing by or ending by

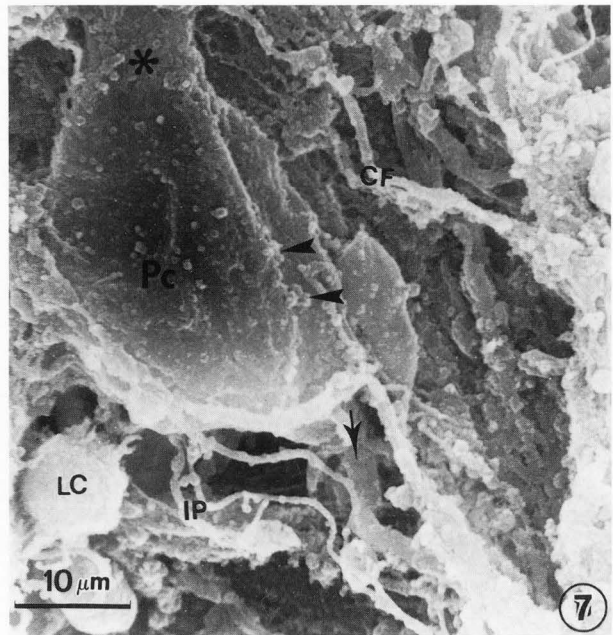


**Figure 7.** Teleost fish cerebellar cortex. Purkinje cell layer. The soma, primary dendritic trunk (asterisk) and axon hillock region (arrow) of a Purkinje cell (Pc) are appreciated. In addition, a partial view of the infra-ganglionic plexus (IP) and ascending climbing fiber (CF) are observed. Vestiges of Bergmann glial cell cytoplasm (arrowheads) are seen attached to the Purkinje cell outer surface. A cell (Lugaro cell?) (LC) is observed at the left corner. Freon-freeze fracture method. Gold-palladium coating.

means of bulbous endings upon the surface of Purkinje cell tertiary dendritic shafts or in their spines (Fig. 3). According to the uniform caliber of the parent fiber, intracortical course, topographical relationship with Purkinje cell dendrites and presence of fine ramifications, the parent fibers and their collateral processes were interpreted as climbing fibers.

The mossy fibers were observed as thick parent fibers entering into successive granule cell groups in the granular layer and establishing *en passant* relationship with several groups of granule cells (Fig. 4).

### SEM freeze-fracture method

Since the slicing technique for SEM does not allow us to accurately differentiate climbing fibers from mossy fibers, we applied the freeze fracture SEM method of Humphreys *et al.* (1974, 1975) in order to obtain new views of interneuronal relationship and expose hidden neuronal surfaces. At the level of the granular layer, the cerebellar glomerulus was fractured exposing the interior of the granule cell groups and the intimate relationship of granule cell dendrites with the varicosities or

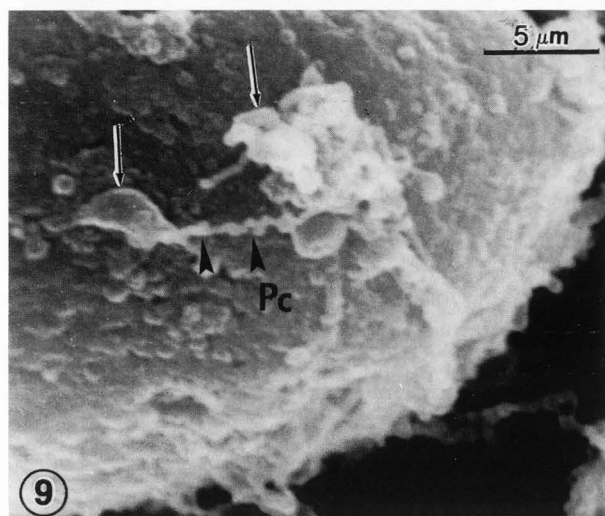
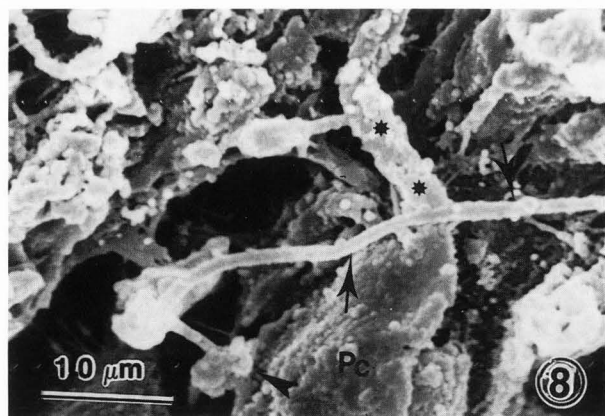


**Figure 8.** Human edematous cerebellum. Purkinje cell layer. A transversely running axon (arrows) is observed crossing the upper pole cell body of a Purkinje cell (Pc) and establishing an axosomatic contact (arrowhead) with the Purkinje cell somatic outer surface. Ethanol-cryofracturing technique. The asterisks label the primary dendritic trunk. The removed Bergmann glial cytoplasm occupied the dark spaces surrounding the Purkinje cell. Gold-palladium coating.

**Figure 9.** Human edematous cerebellum. Purkinje cell (Pc) somatic outer surface. Fractured axo-somatic basket cell endings (arrows) are observed interconnected (arrowheads) and attached to the Purkinje cell somatic outer surface. The ethanol-cryofracturing process has sectioned the incoming basket cell axons and removed the satellite Bergmann glial cell cytoplasm. Gold-palladium coating.

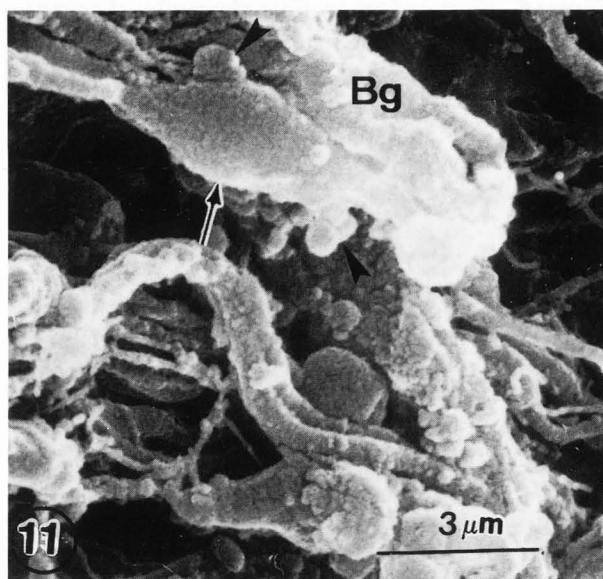
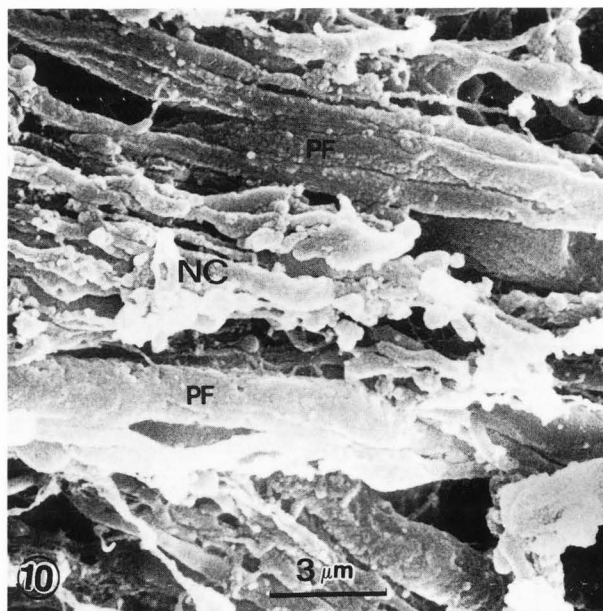


**Figure 10.** Teleost fish cerebellar cortex. Molecular layer. Outer surface of bundles of parallel fibers (PF) and vestiges of attached neuroglial cytoplasm (NC). The non-synaptic segment of parallel fiber shows uniform caliber. Gold-palladium coating.

**Figure 11.** Teleost fish cerebellum. Molecular layer. Parallel fiber showing the synaptic varicosity (arrow) in contact with the *en face* view of a Purkinje dendritic spine body (arrowhead). The satellite Bergmann glial cell cytoplasm (Bg) is also seen. Gold-palladium coating.

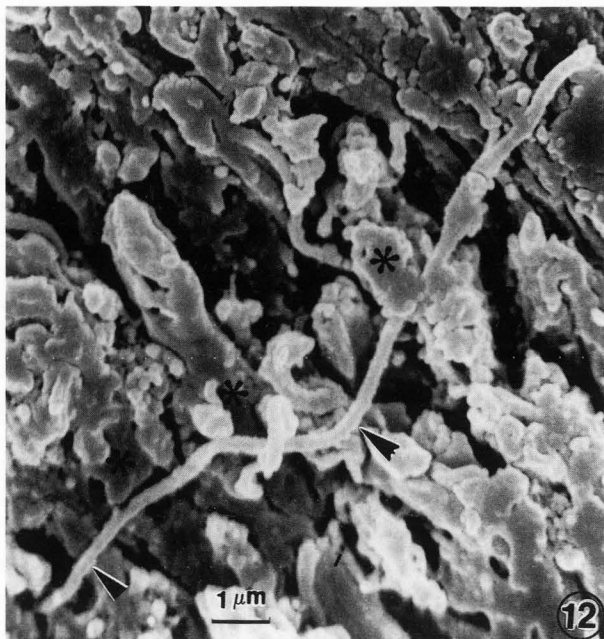


**Figure 12.** Human edematous cerebellar cortex. Molecular layer. A parallel fiber is observed making *en passant* axo-dendritic contacts (arrowheads) with successive Purkinje dendritic branchlets (asterisks). The ethanol cryofracturing technique has removed the enveloping neuroglial cytoplasm. Gold-palladium coating.

rosettes of mossy fibers (Fig. 5). Another fractured mossy glomerulus showed a group of granule cells with their dendritic processes radially converging onto the central mossy rosette expansion (Fig. 6). In this case, up to 18 granule cells were observed sending their dendrites to the mossy rosette, which gave an idea of the degree of divergent information at the level of each mossy glomerulus. These observations clearly differentiate mossy fiber (1 to 18 ratio) from climbing fiber (1 to 1 ratio) relations with granule cell dendrites.

At the level of Purkinje cell layer, the cryofracture process removed the satellite Bergman glial cell, a regional protoplasmic astrocyte covering the Purkinje cell, exposing the surface of a Purkinje cell body, the emergence of the primary dendritic trunk and the axon hillock region (Fig. 7). In addition, a partial view was obtained of the infraganglionic plexus of a Purkinje cell and neighboring cells, presumably basket cells. Examination of the upper pole body of a Purkinje cell, at the site of emergence of the primary dendritic trunk, permitted us to observe in human cerebellum, the transversally running basket cell axons establishing axosomatic contacts with a Purkinje cell somatic surface (Fig. 8). These axons form part of the so-called supraganglionic plexus of Purkinje cells. A further exploration of the Purkinje cell somatic outer surface revealed attached

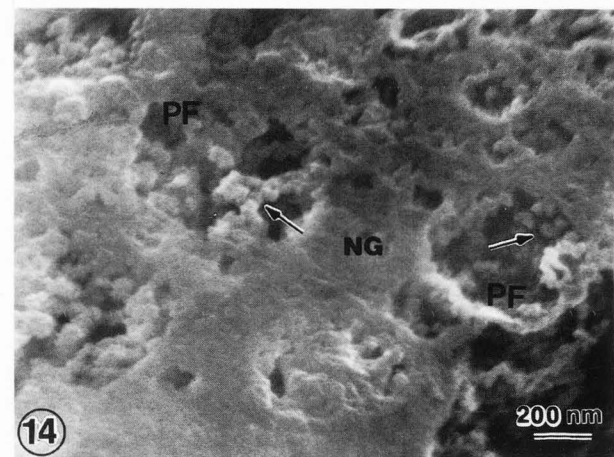
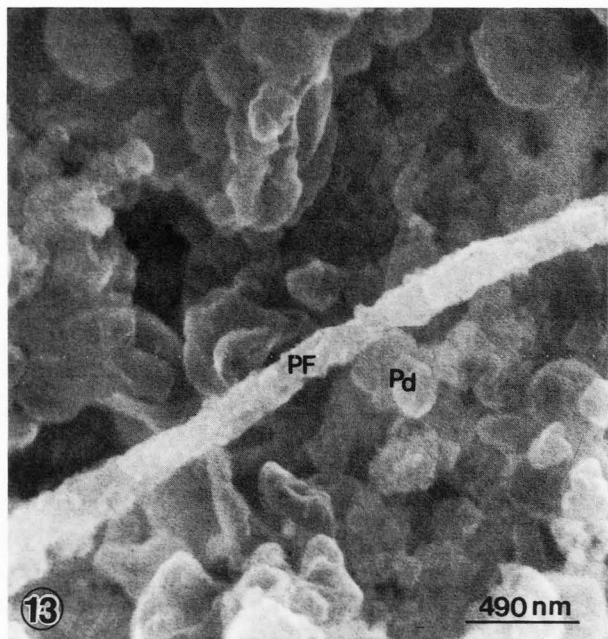


**Figure 13.** Rhesus monkey cerebellar cortex. Molecular layer. A non-synaptic segment of parallel fiber (PF) is observed crossing the spiny surface of a Purkinje tertiary dendritic branch (Pd). The high resolution scanning electron microscopy and chromium coating gave a high material density to the parallel fiber and a gray, less dense appearance to the dendritic surface. Compare the improved quality image with the previous figures.

**Figure 14.** Rhesus monkey cerebellar cortex. Molecular layer showing two fractured synaptic varicosities of parallel fiber (PF) with clustered spheroidal synaptic vesicles (arrows), which appeared surrounded by neuroglial cell cytoplasm (NG).

axosomatic boutons (Fig. 9). Apparently, the cryofracture process sectioned the incoming fibers and separated the neuroglial sheath of Purkinje cells, thus exposing the axosomatic contacts.

At the level of the molecular layer, examination of teleost fish cerebellum with the conventional SEM showed the longitudinal profiles of the non-synaptic segments of parallel fibers (Fig. 10). They appeared as longitudinally running bundles partially separated by vestiges of intervening Bergmann glial cell cytoplasm.

The parallel fibers showed fusiform varicosities or synaptic enlargements at the level of the contacts with the Purkinje cell dendritic spines (Fig. 11). Scanning the molecular layer of human cerebellum, we were able to characterize the *en passant* nature of the parallel fiber axospinodendritic synaptic contacts with successive Purkinje cell dendrites (Fig. 12). Parallel fibers appeared transversely running in the molecular layer, whereas the Purkinje cell dendrites appeared longitudinally ascending configuring "cruciform" or "crossing over" synapses.

In primate cerebellar molecular layer, a more detailed view of the non synaptic region of parallel fiber and the outer surface of Purkinje tertiary dendrites was obtained (Fig. 13). In this case, using the delicate specimen preparation, the chromium coating, and the instrumental parameter of a high resolution electron microscope, permitted us to obtain an SE-I image of the outer surface of axons and dendritic processes, revealing the brilliant mass density of the axonal profiles and the gray, less dense smooth spiny surface of tertiary dendritic outer surfaces.

Cross-sectioned parallel fiber synaptic varicosities contained the spheroidal synaptic vesicles (Fig. 14) and appeared surrounded by Bergman glial cell neuroglial cytoplasm.

### Discussion

In the present paper, we have demonstrated that the slicing technique and the cryofracture method for SEM have some potential value for exposing the nerve cell circuits within a central gray nerve center. In the slicing technique, the plane of the section can be orientated for obtaining the desired sagittal, transverse or *en face* sections of the cerebellar folia. With the cryofracture methods, either by liquid nitrogen (Humphreys *et al.*, 1974) or freon 22 (Apkarian and Curtis, 1986), the cleavage plane is randomly obtained. However, the irregular fracture surface permits an in depth analysis of the course of a particular nerve process. In the exploration of the intracortical course of an afferent fiber or an intrinsic fiber, we have taken advantage of the high resolution and large depth of focus of conventional and

high resolution scanning electron microscopes, which allow continuous exploration of nerve processes throughout the multilayered structure of the gray center. The cleavage plane is often produced at the intercellular level during the cryofracture process with liquid nitrogen (medium freezing rate), removing the neuroglial cytoplasm covering the neuronal surface and the nerve cell processes. This exposes the trajectory of the almost intact nerve cell circuits and interconnections and facilitates exploration with the scanning electron microscope probe. Since nerve tissue forms a compact neuropil, the fractured surface exposed hidden surface but unfortunately broke some interconnections. This limitation should be taken into consideration in identifying a particular nerve fiber, since it alters the degree of lateral collateralization, a criterion which is important in the identification of a nerve fiber.

The criteria of identification used in the present study took into consideration previous descriptions with the Golgi optical microscope and thin section transmission electron microscope (TEM) studies combined with three-dimensional reconstruction.

In the identification of climbing fibers in the cerebellar cortex, the following features were considered: **a)** caliber of fibers (thinner than mossy fibers), **b)** intracortical course through the cerebellar cortex given by previous Golgi light microscope studies (Scheibel and Scheibel, 1954; Ramón y Cajal, 1955), combined Golgi and TEM studies (Palay and Chan-Palay, 1974), and different SEM methodology, such as the ashing technique (Lewis, 1971), creative tearing technique (Scheibel *et al.*, 1981) or ultrasonic micro-dissection (Low, 1989); **c)** degree of collateralization in the granular layer (Palay and Chan-Palay, 1974) and in the molecular layer (Scheibel and Scheibel, 1954; Castejón, 1983, 1986; Castejón and Castejón, 1987). In this context, scanning electron microscopy should be considered as a complementary and powerful exploration technique that requires previous knowledge from related microscopic techniques for proper orientation and interpretation.

For the identification of mossy fibers, we have taken into account the following features: **a)** larger caliber than climbing fibers (Mugnaini, 1972); **b)** classically described endings in the granular layer and typical rosette formations (Ramón y Cajal, 1955; Palay and Chan-Palay, 1974); **c)** glomerular type of engagement with multiple granule cell dendrites; **d)** dichotomous branching pattern (Castejón, 1991), contrasting with the "cross-over" bifurcation pattern of climbing fibers (Castejón and Castejón, 1987).

For the identification of fine delicate ramifications of the mossy and climbing fibers in the granular layer, we have ascertained that there is a source of confusion with the highly branched axonal ramification of Golgi

cell axons. In this case, the small area of the fracture surface limits scanning of the connection with the parent fibers and impedes a proper identification.

The freeze-fracture method for SEM made it possible to obtain an inner view of the mossy fiber glomerulus, complementing the information obtained with TEM, either by thin sections (Mugnaini, 1972) or freeze-etching replicas (Castejón, 1991). In addition, it seemed to establish the quantitative relation between granule cells and the mossy fiber rosettes. The mossy rosette-granule cell ratio is 1 to 15 (Fox *et al.*, 1967) or 1 to 20 (Eccles *et al.*, 1967), as estimated by Golgi light microscope studies. This ratio gives an idea of the degree of divergence of information on each mossy glomerulus. A systematic study with SEM could provide with a major degree of accuracy the exact degree of divergence. In a previous study (Castejón, 1991), we have preliminarily estimated a ratio of 1 to 18. The inner view of mossy glomerulus with the SEM cryofracture method opens new lines of research on quantitative analysis of glomerular synapses.

Conventional scanning electron microscopy, in which the specimen is staged at a working distance below the final probe forming lens and using 5-10 nm gold-palladium coated samples, has provided for the first time, the outer surface image of cerebellar parallel fibers and confirmed the "crossing-over" type, and *en passant* nature, of parallel fiber-Purkinje cell dendrite synaptic relationship, as earlier described by TEM studies (Hamori and Szentagothai, 1964). In this synaptic relationship, as illustrated in Fig. 13, the HRSEM with the "in lens" position of the specimen and the ultrathin chromium coating have provided a close approximation to the true outer nerve cell process surface, allowing us to study spine synaptic relationship (Castejón and Apkarian, 1993). In this context, HRSEM offers new perspectives on the study of spine synaptic morphology.

In the high resolution scanning electron microscope, an efficient detector placed above the condenser/objective (C/O) lens specimen stage along with a high brightness LaB<sub>6</sub> or a field emission (FE) emitter creates a condition of specimen collection specifically useful for imaging SE-I contrast (Apkarian, 1989). This new methodology could be used for tracing the final endings of extrinsic or intrinsic nerve fibers. As shown in Figure 14, the inner surface morphology of a presynaptic ending could be obtained. The thinner chromium coating used (2 nm thick) allowed us to obtain the relief contrast of the limiting plasma membrane profile and the outer surface morphology of synaptic vesicles. This circumstance will make it possible, in the future, to obtain a higher magnification of the three-dimensional macromolecular architecture of synaptic membranes.

## References

- Anderson RF (1951) Techniques for the preservation of three-dimensional structure in preparing specimens for the electron microscope. *Trans Acad Sci (New York)* **13**, 130-134.
- Apkarian RP, Curtis JC (1986) Hormonal regulation of capillary fenestrae in the rat adrenal cortex: Quantitative studies using objective lens staging scanning electron microscopy. *Scanning Electron Microsc* **1986**; IV: 1381-1393.
- Apkarian RP (1989) Conditions required for detection of specimen specific SE-I secondary electrons in analytical SEM. *J Microsc* **154**, 177-188.
- Apkarian RP (1994) Analysis of high quality monatomic chromium films used in biological high resolution scanning electron microscopy. *Scanning Microsc* **8**, (this issue).
- Castejón OJ (1981) Light microscope, SEM and TEM study of fish cerebellar granule cells. *Scanning Electron Microsc* **1981**; IV, 105-113.
- Castejón OJ (1983) Scanning electron microscope recognition of intracortical climbing fiber pathways in the cerebellar cortex. *Scanning Electron Microsc* **1983**; III, 1427-1434.
- Castejón OJ (1984) Low resolution scanning electron microscopy of cerebellar neurons and neuroglial cells of the granular layer. *Scanning Electron Microsc* **1984**; III, 1391-1400.
- Castejón OJ (1986) Freeze-fracture of fish and mouse cerebellar climbing fibers. A SEM and TEM study. *Electron Microscopy, Vol. IV*. Imura T, Maruse S, Suyuki T (Eds). Japanese Society of Electron Microscopy. Tokyo, Japan. pp. 3165-3166 (abstract).
- Castejón OJ (1988) Scanning electron microscopy of vertebrate cerebellar cortex. *Scanning Microsc* **2**, 569-597.
- Castejón OJ (1990a) Freeze-fracture scanning electron microscopy and comparative freeze-etching study of parallel fiber-Purkinje spine synapses of vertebrate cerebellar cortex. *J Submicrosc Cytol Pathol* **22**, 281-295.
- Castejón OJ (1990b) Scanning electron microscopy study of cerebellar synaptic junctions. In: *Electron Microscopy 1990*. San Francisco Press, San Francisco. pp. 148-149 (abstract).
- Castejón OJ (1991) Three-dimensional morphological analysis of nerve cells by scanning electron microscopy. A review. *Scanning Microsc* **5**, 461-476.
- Castejón OJ (1993) Sample preparation techniques for conventional and high resolution scanning electron microscopy of the central nervous system. The cerebellum as a model. *Scanning Microsc* **7**, 725-740.
- Castejón OJ, Apkarian RP (1992) Conventional and high resolution scanning electron microscopy of outer

and inner surface features of cerebellar nerve cells. *J Submicrosc Cytol Pathol* **24**, 549-562.

Castejón OJ, Apkarian RP (1993) Conventional and high resolution field emission scanning electron microscopy of vertebrate cerebellar parallel fiber-Purkinje spine synapses. *Cell Mol Biol* **39**, 863-873.

Castejón OJ, Caraballo AJ (1980) Application of cryofracture and SEM to the study of human cerebellar cortex. *Scanning Electron Microsc* **1980**; IV, 197-207.

Castejón OJ, Castejón HV (1987) Scanning electron microscope, freeze-etching and glycosaminoglycan cytochemical studies of the cerebellar climbing fiber system. *Scanning Microsc* **2**, 2181-2193.

Castejón OJ, Valero C (1980) Scanning electron microscopy of human cerebellar cortex. *Cell Tissue Res* **212**, 363-374.

Eccles J, Ito M, Szentagothai J (1967) *The Cerebellum as a Neuronal Machine*. Springer-Verlag, New York, pp 116-156.

Fox CA, Hillman DE, Siegesmund KA, Dutta CR (1967) The primate cerebellar cortex: A Golgi and electron microscopic study. *Prog Brain Res* **25**, 174-225.

Haggis GH (1970) Cryofracture of biological material. *Scanning Electron Microsc* **1970**, 97-104.

Haggis GH, Phipps-Todd B (1977) Freeze-fracture scanning electron microscopy. *J Microsc* **111**, 193-201.

Hamori J, Szentagothai J (1964) The "crossing-over" synapses. An electron microscope study of the molecular layer on the cerebellar cortex. *Acta Biol Sci Hung* **15**, 95-117.

Humphreys WJ, Spurlock BO, Johnson JS (1974) Critical point drying of ethanol-infiltrated cryofracture biological specimens for scanning electron microscopy. *Scanning Electron Microsc* **1974**, 276-282.

Humphreys WJ, Spurlock BO, Johnson JS (1975) Transmission electron microscopy of tissue prepared for scanning electron microscopy by ethanol-cryofracturing. *Stain Tech* **50**, 119-125.

Kuffler SW, Nicholls JG, Martin AR (1984) *From Neuron to Brain. A Cellular Approach to the Function of the Nervous System*. Sinaver Assoc Inc Pub., Sunderland, Mass. USA. pp. 75-96.

Lewis RE (1971) Studying neuronal architecture and organization with the scanning electron microscope. *Scanning Electron Microsc* **1971**, 283-288.

Llinas R, Hillman DE (1969) Physiological and morphological organization of the cerebellar circuits in various vertebrates. In: *Neurobiology of Cerebellar Evolution and Development*. Llinas R (ed). AMA-ERF Institute for Biomedical Research, Chicago. pp. 43-73.

Low FN (1989) Microdissection by ultrasonication for scanning electron microscopy. In: *Cells and Tissue: A Three-Dimensional Approach by Modern Techniques in Microscopy*. Alan R Liss Inc., New York. pp. 571-

580.

Mugnaini E (1972) The histology and cytology of the cerebellar cortex. In: *The Comparative Anatomy and Histology of the Cerebellum. The Human Cerebellum. Cerebellar Connections and Cerebellar Cortex*. Larsell O, Jansen J (eds.). The University of Minnesota Press, Minneapolis, MN. pp. 201-251.

Palay SL, Chan-Palay V (1974) Methods. In: *Cerebellar Cortex. Cytology and Organization*. Springer-Verlag, Berlin. pp. 322-336.

Peters KR (1980) Improved handling of structural fragile cell-biological specimens during electron microscopic preparation by the exchange method. *J Microsc* **118**, 429-441.

Peters KR (1985) Noise reduction in high magnification micrographs by soft focus printing and digital image processing. *Scanning* **7**, 205-215.

Ramón y Cajal S (1955) *Histologie du Système Nerveux de l'Homme et des Vertèbres (Histology of the nervous system of humans and vertebrates)*. Vol 2. Consejo Superior de Investigaciones Científicas, Instituto Ramón y Cajal, Madrid, Spain. pp. 55-79.

Scheibel ME, Scheibel AB (1954) Observations on the intracortical relations of the climbing fibers of the cerebellum. *J Comp Neurol* **101**, 733-763.

Scheibel AB, Paul LA, Fried I (1981) Scanning electron microscopy of the central nervous system. I: The Cerebellum. *Brain Res Rev* **3**, 207-228.

Shepher GM (1988) *Neurobiology*. Oxford University Press, New York. pp. 145-175.

#### Discussion with Reviewers

**P. Mestres:** In general, the SEM equipped with field emission gun (FEG) is advantageous in biology working at low voltage. Why do you use FEG at higher voltages (30 kV)?.

**Authors:** We are using FEG at high voltage because at the present time, we are interested in tracing the fine, delicate afferent nerve fiber endings making surface contacts with dendritic outer surface. In addition, we want to show the inner surface of the cross-fractured synaptic endings. The S-900 at 30 kV has a theoretically predicted probe diameter of 0.5 nm [Nagatani T, Saito S, Sato M, Yamada M (1987). Development of an ultra-high resolution scanning electron microscope by means of a field emission source and in-lens system. *Scanning Microsc*. **1**, 901-909] and shows a resolution of significant biological structures 2-5 nm in diameter. In the future, when dealing with macromolecular imaging of neuronal membranes, we will use FEG below 4 kV in order to obtain better topographic contrast and even better resolution.